Finite Amplitude Shear Wave Instabilities

H. Tuba Özkan and James T. Kirby [1]

Abstract

The growth to finite amplitude of instabilities in a longshore current is studied using a two dimensional horizontal model of the continuity and momentum equations. Spatial derivatives contained in these equations are computed using spectral collocation methods. A high-order time integration scheme is incorporated to compute the time evolution of the velocities and water surface elevation given initial conditions. The model domain extends from the shoreline to a finite distance offshore and is finite in the longshore direction. A curvilinear moving boundary condition is incorporated at the shoreline and is tested using solutions for one and two dimensional wave runup. A transmitting boundary is constructed offshore and periodicity is assumed on the longshore boundaries. The model is then utilized to study the nonlinear evolution of shear waves on a plane beach. It is seen that in this environment, long term evolution of the shear wave is strongly dominated by subharmonic transitions that give flow structures that could be characterized as migrating rip currents.

Introduction

Shear waves were first identified in field data from the SUPERDUCK experiment. Data from this experiment showed the presence of energetic, longshore-progressive wave-like disturbances that typically have frequencies that fall in the lower range of the infra-gravity band and wavenumbers that are much larger than that of a mode zero edge wave (Oltman-Shay *et al.*, 1989). The wavenumber-frequency spectrum of the measured longshore velocity in the SUPERDUCK experiment (see Figure 1a) shows the range in which these disturbances occur and their non-dispersive character. A look at the time series of the longshore velocity (see Figure 1b) also confirms the presence of these low frequency oscillations. More recently, these waves have also been observed in the laboratory (Reniers *et al.*, 1994).

[1]Center for Applied Coastal Research, Ocean Engineering Lab, University of Delaware, Newark, DE 19716

Bowen and Holman (1989) constructed a linearized analytical model by assuming a simplified bottom topography and current field, inviscid flow and a rigid lid and attributed these disturbances to instabilities in the longshore current. These instabilities were found to be possibly linked to the seaward shear of the longshore current profile and were, therefore, termed shear waves. Subsequent investigators such as Dodd *et al.* (1992), Putrevu and Svendsen (1992), Dodd and Thornton (1992), Dodd (1994), Falqués and Iranzo (1994), Falqués *et al.* (1994) and Allen *et al.* (1995) worked on lifting the limitations on Bowen and Holman's (1989) model.

Figure 1: (a) Wavenumber-frequency spectrum for longshore velocity, SUPERDUCK field experiment (b) Time series of longshore velocity (from Oltman-Shay *et al.*, 1989).

Returning to Figure 1, it can be noted that signatures of a variety of low frequency motions are visible in the wavenumber-frequency spectrum. These include wave induced longshore currents, gravity waves such as edge waves or leaky waves, as well as vorticity waves such as shear waves. The simultaneous presence and importance of all these motions dictates the necessity to formulate a robust and comprehensive model in order to focus on surf zone as well as swash zone dynamics.

Governing Equations

In this study, a two dimensional horizontal model of the short wave averaged continuity and momentum equations is developed. The governing equations, given below, are the shallow water equations with additional terms to include the effects of temporally and spatially varying forcing due to incident waves and

damping in the form of bottom friction.

$$\begin{aligned}
&\eta_t + [u(h+\eta)]_x + [v(h+\eta)]_y = 0 \\
&u_t + uu_x + vu_y = -g\eta_x + \tau_x - \frac{\mu}{h}u \\
&v_t + uv_x + vv_y = -g\eta_y + \tau_y - \frac{\mu}{h}v
\end{aligned} \tag{1}$$

Here, η is the water surface elevation above the mean water level, h is the still water depth, u and v are the short wave averaged velocity components in the x and y directions, respectively, where x points offshore and y points in the longshore direction. The parameters τ_x and τ_y represent the effect of short wave forcing in the x and y directions, respectively. Furthermore, a linear bottom friction term is incorporated in both horizontal directions.

The domain in which these equations are solved is bounded by a curvilinear moving shoreline at $x = \zeta(y,t)$ and by an open boundary at $x = L_x$. The breaker line is denoted by L. Periodicity is assumed in the y direction.

It is more convenient to impose the onshore and offshore boundary conditions if the governing equations are written in characteristic form. Algebraic manipulation of the continuity and momentum equations results in three equations in the unknown characteristic variables β_1, β_2, and γ.

$$\begin{aligned}
\beta_{1_t} + (u-c)\beta_{1_x} + v\beta_{1_y} - cv_y &= 2c_0c_{0x} + \tau_x - \frac{\mu}{h}u \\
\beta_{2_t} + (u+c)\beta_{1_x} + v\beta_{2_y} + cv_y &= 2c_0c_{0x} + \tau_x - \frac{\mu}{h}u \\
\gamma_t + u\gamma_x + v\gamma_y &= -g\eta_y + \tau_y - \frac{\mu}{h}v.
\end{aligned} \tag{2}$$

Here, c is the nonlinear shallow water wave speed $\sqrt{g(h+\eta)}$ and c_0 is the linear shallow water wave speed $\sqrt{gh}$. Note that in the absence of longshore variability, forcing and damping, the above equations reduce to uncoupled one-way wave equations. The characteristic variables are given by $\beta_1 = u - 2c$ traveling in the $-x$ direction, $\beta_2 = u + 2c$ traveling in the $+x$ direction, and $\gamma = v$ traveling in the $\pm y$ direction.

Treatment of Moving Shoreline

The problem at hand consists of solving a set of well-known governing equations in a complicated physical domain bounded by one curvilinear moving boundary and three stationary boundaries. However, the variable physical domain can be mapped onto a new stationary domain using a simple coordinate transformation. Hence, the problem can be reduced to solving the set of governing equations with some extra terms in a rectangular domain with four stationary boundaries—a much simpler task.

The coordinate transformation from the physical variables $x \in [\zeta(y,t), L_x]$ and $y \in [0, L_y]$ to the intermediate variables $\phi \in [0, L_x]$ and $\psi \in [0, L_y]$ used here

is given by

$$x = \phi + \zeta(y,t)e^{-\alpha\phi^2}, \qquad y = \psi. \tag{3}$$

A stationary orthogonal grid in the (ϕ, ψ) domain corresponds to a physical grid that is following the shoreline (see Figure 2). The movement of the grid is damped out exponentially with offshore distance so that the grid is stationary at a certain distance offshore which is dictated by the value of the parameter α. At locations further offshore, the physical grid and the intermediate grid are identical. As a result of the transformation, the derivatives in the governing equations are altered, resulting in a few additional terms.

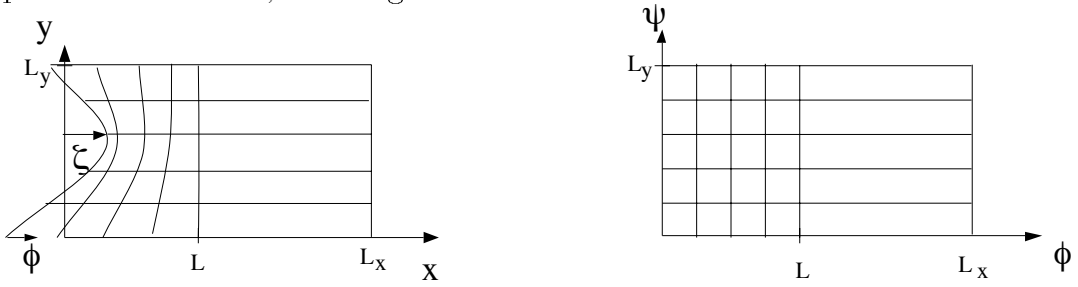

Figure 2: Shoreline Boundary Condition: Transformation from the physical to the intermediate domain

The intermediate grid in the variables $\phi \in [0, L_x]$ and $\psi \in [0, L_y]$ obtained above is at this step mapped onto a computational grid in the variables $s \in [-1, 1]$ and $r \in [0, L_y]$. The coordinate transformation

$$\phi = L\frac{1+s}{s_0 - s}, \qquad \psi = r \tag{4}$$

is used. The value of the parameter s_0 is dictated by the location of the offshore boundary. If the offshore boundary is located at infinity s_0 equals unity. In this case a physical domain in the shape of a semi-infinite strip is modeled while the computations are carried out in a box-shaped domain. On the other hand, for a finite offshore width $s_0 > 1$.

Offshore Open Boundary Condition

Any wave reaching the offshore boundary should be allowed to leave the domain with no or minor reflection. Therefore, a transmitting boundary condition must be used. In this study the treatment of the offshore boundary is carried out following Van Dongeren *et al.* (1994), who reported reflection coefficients on the order of 0.1%. The method is applied with only minor modifications. A brief summary will be given here; the reader is referred to Van Dongeren *et al.* (1994) and the references therein for details.

The particle velocity $\vec{U}$ associated with an outgoing wave can be expressed in terms of its offshore component u and longshore component v. Known quantities

at the boundary are the longshore characteristic $\gamma = v$ and the outgoing characteristic $\beta_2 = u+2c$. However, the incoming characteristic $\beta_1 = u-2c$ is unknown as u and c are unknown. By assuming that the outgoing wave is of permanent form, we can impose a condition on the particle velocity: $|\vec{U}| = 2c - 2c_0$. Using the geometric argument $|\vec{U}|^2 = u^2 + v^2$ we can then write

$$4(c - c_0)^2 = u^2 + v^2. \tag{5}$$

Also using

$$\beta_2 = u + 2c \tag{6}$$

the resulting system of two equations in the two unknowns u and c can be straightforwardly solved and the incoming characteristic $\beta_1 = u - 2c$ can be specified at the offshore boundary.

Numerical Method

Given an initial condition in the water surface elevation η and the velocities u and v, the governing equations are integrated in time using an explicit third order Adams-Bashforth scheme. The spatial derivatives in the horizontal directions are computed using a spectral collocation scheme. One advantage to using such a scheme is the increased accuracy of the solution since no truncation errors (i.e. dispersion or dissipation errors) are made. Another advantage is the rapid spectral convergence of the solution. The error in the solution is approximately halved when an additional grid point is added. In contrast, the use of finite difference schemes requires doubling the number of grid points in order to halve the error.

Fourier collocation is used in the longshore direction r with equally spaced collocation points. Chebyshev collocation is used in the offshore direction s. The collocation points s_i (i = 1, ...,N) are chosen as the reversed Gauss-Lobatto points given by $s_i = -\cos\frac{\pi i}{N}$. This choice ensures that the grid points in the physical domain are concentrated within the surf zone with the highest concentration close to the shoreline.

Falqués and Iranzo (1992, 1994) have applied Chebyshev collocation in conjunction with Fourier collocation to several low frequency surf zone motions and reported the adequacy and efficiency of the method for edge wave or shear wave calculations.

Applications

In this section an analytical solution for a single wave runup on a sloping beach by Carrier and Greenspan (1958) is used to verify the accuracy of the shoreline treatment. In this simulation the model domain extends to infinity in the offshore direction. Figure 3a shows snapshots of the water surface elevation

η as a function of offshore distance every 1.6 seconds, with $t = 0$ sec corresponding to the maximum rundown position and $t = 19.2$ sec corresponding to the maximum runup position. The comparison with the exact solution is very good.

The second application involves solitary wave runup on a bay with a sloping bottom. Computations for this case have previously been carried out by Zelt (1986) using a fully Lagrangian finite element model, and results show pronounced two dimensional runup. Figure 3b shows time series of the runup in the cross-shore direction at different locations along the bay, where $y = 0$ denotes the midpoint of the bay. The present model compares well with the numerical solution by Zelt (1986).

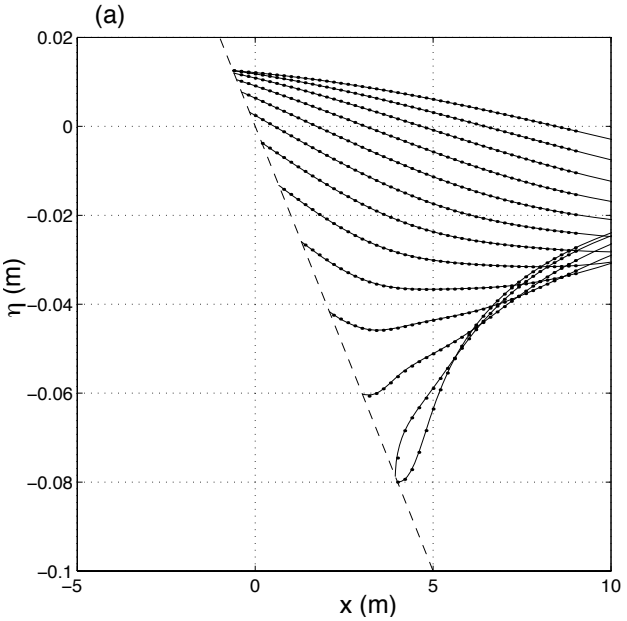

Figure 3: (a) Runup in 1D: Snapshots with $\Delta t = 1.6$ sec of η versus x. Exact solution (dotted), present model (solid).
(b) Runup in 2D: Time series of runup along y. Zelt (solid), present model (dashed).

Instabilities in the Longshore Current

In order to simulate growth of shear waves to finite amplitude, a plane beach geometry with a slope of $m = 0.05$ is chosen. This bottom slope is similar to an average slope of the bathymetry at SUPERDUCK. Furthermore, this bathymetry has also been used by Allen *et al.* (1995) in conjunction with a frictionally balanced current profile in the form

$$V(x) = Cx^2 \exp\{-\left(\frac{x}{\alpha}\right)^3\}, \tag{7}$$

with the parameters C and α chosen such that a maximum current velocity of 1 m/s occurs at $x = 90$ m. Linear instability calculations for this bathymetry

and current profile show that the wavelength λ associated with the most unstable mode is 450 m.

The current profile given in Equation (7) is also adopted in the present study so that comparisons to Allen *et al.* 's (1995) results can be made. Such comparisons will aid in the identification of the importance of the rigid lid assumption, which is used in Allen *et al.*'s (1995) study but not in the present study. It should be noted that the bottom and current profiles are not compatible but, nevertheless, are expected to convey an idea about the main features of the instability.

In this study, a fixed friction coefficient μ of 0.006 m/s is used. This value was chosen in light of results by Dodd *et al.* (1992) and Allen *et al.* (1995). The offshore boundary is placed at $L_x = 360$ m. The width of the domain in the longshore direction is set such that

$$L_y = ND \times \left(\frac{2\pi}{k}\right), \tag{8}$$

where k is the linearly most unstable wavenumber given by $(2\pi/\lambda)$ and ND is an integer. Due to the periodicity condition in the y direction, the choice of ND dictates the wavenumbers that can exist in the domain. For $ND = 1$ only the most unstable wavenumber k and its harmonics can exist in the domain. If $ND = 2$ is used, waves with wavenumbers $k/2, 3k/2, 5k/2, \ldots$ are also allowed to exist. Therefore, as ND is increased, the wavenumber spectrum is more densely populated, effectively simulating a continuous spectrum.

The initial condition to the model is obtained using the linear solution by Putrevu and Svendsen (1992) for the perturbation velocities u_l and v_l. The initial velocities and water surface elevation are then prescribed as follows:

$$\begin{aligned} u(x,y,0) &= \epsilon u_l(x,y) \\ v(x,y,0) &= V(x) + \epsilon v_l(x,y) \\ \eta(x,y,0) &= 0, \end{aligned} \tag{9}$$

where ϵ is of $O(10^{-3})$.

Information about the longshore scale of the motion can be obtained by investigating the effect of the chosen domain width. This is achieved by successively increasing ND. In the following, time series at $(x,y) = (L, 0.5L_y)$, contour plots of the potential vorticity

$$q = \frac{v_x - u_y}{h + \eta} \tag{10}$$

and plots of circulation patterns will be shown for ND =1,2 and 4.

Results for $L_y = 1 \times (2\pi/k)$.

Time series of u, v and η at $x = L$ and $y = 0.5L_y$ given in Figure 4 show that the initial perturbations in the most unstable mode grow to finite amplitude

and form a final steady wave of modulated amplitude. It can be seen that the initial perturbations in u grow to a maximum amplitude of about 20% of the maximum longshore current. This is in agreement with observations in the field and in the laboratory. The perturbations in v grow to an amplitude of about 50% of the maximum longshore current. We can also see a shift in the mean longshore current at this location. The water surface elevation η also grows to a finite amplitude, however this amplitude is very small ($O(1$ mm$)$). All three time series show that the waves with the highest amplitudes have larger periods, suggesting that the larger waves travel slower.

Results for the velocity components are in quantitative agreement with those by Allen *et al.* (1995) obtained using the rigid lid assumption. The results also qualitatively correspond to computations carried out by Falqués *et al.* (1994) for a different current profile using the rigid lid assumption. As computations in this study show that η only reaches values of $O(1$ mm$)$, it can be concluded that the rigid lid assumption is indeed very reasonable for this case. Therefore, results for the water surface elevation will not be shown in the remainder of this paper.

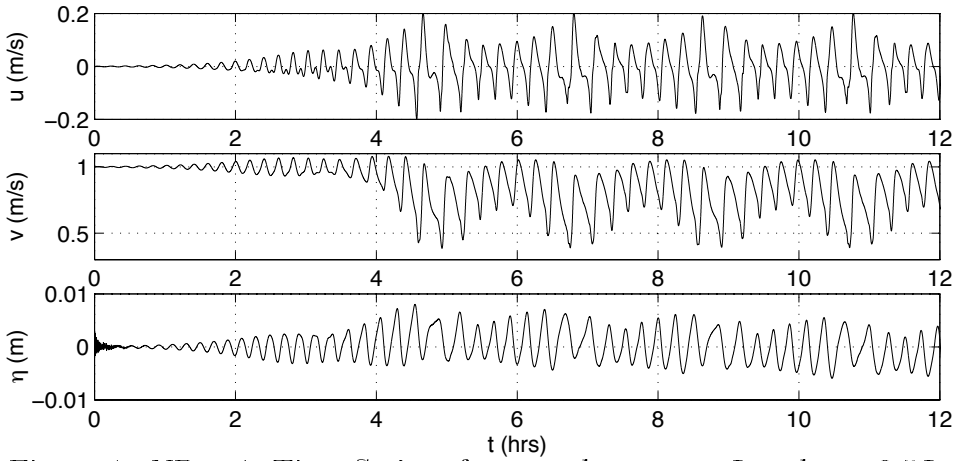

Figure 4: $ND = 1$, Time Series of u, v and η at $x = L$ and $y = 0.5L_y$

Results for $L_y = 2 \times (2\pi/k)$.

In this case the domain is twice as wide as the length of the initially most unstable wave. Therefore, waves with wavenumbers $k/2, k, 3k/2, 2k, \ldots$ can exist in the domain. Time series of u and v given in Figure 5 show that the behavior is initially very similar to that of the previous case. The amplitudes equilibrate and form a final steady wave of modulated amplitude. However, after about three modulation cycles at $t \approx 9$ hrs. these waves undergo a subharmonic transition and evolve into propagating disturbances with the wavenumber $k/2$.

This evolution can be observed in the sequence of snapshots given in Figure 6. This figure depicts contour plots of the potential vorticity as well as plots of the circulation pattern. The disturbances in these plots are traveling in the $+y$ direction. It can be seen that one of the two disturbances develops a larger

amplitude and consequently slows down. The smaller amplitude disturbance behind it catches up with the larger amplitude disturbance and merges into it, forming a circulation pattern with strong offshore directed flow.

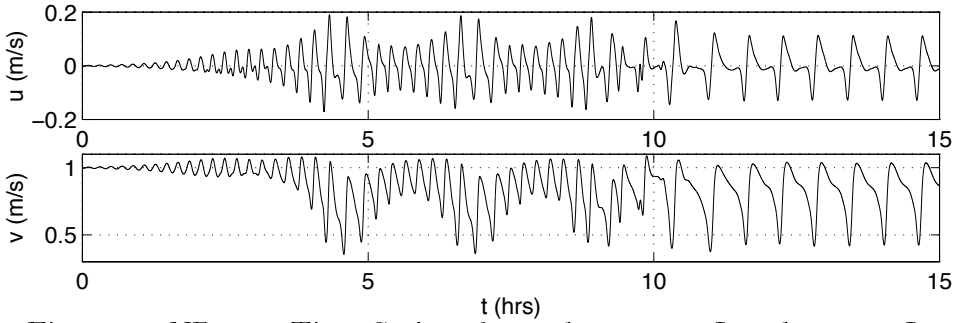

Figure 5: $ND = 2$, Time Series of u and v at $x = L$ and $y = 0.5L_y$

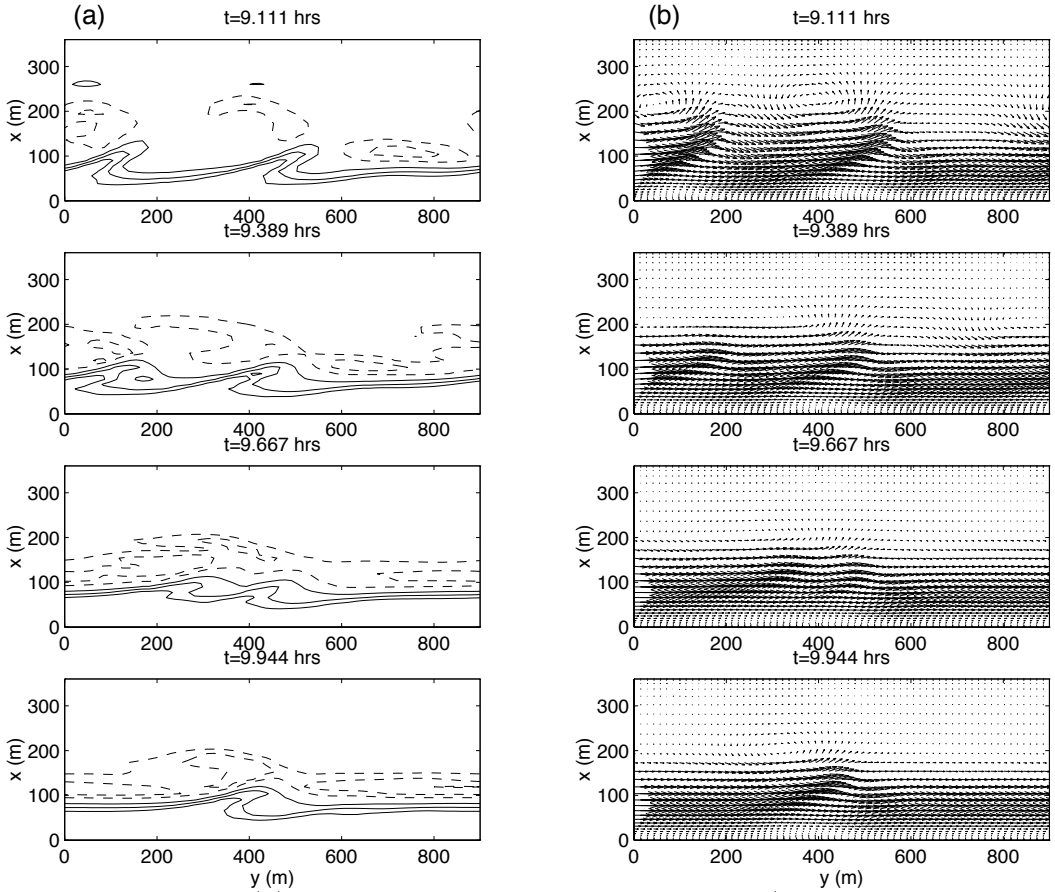

Figure 6: $ND = 2$, (a) Contour plot of potential vorticity (solid for $q > 0$, dashed for $q < 0$) (b) Circulation pattern

Results for $L_y = 4 \times (2\pi/k)$.

Now the domain is four times as wide as the length of the initially most unstable wave. Figure 7 shows the growth of the initially most unstable wavenumber. Again, we observe that waves with higher amplitudes have longer periods. In

this case the subharmonic transition takes place earlier ($t \approx 5$ hrs.). It is evident from the time series and spatial representations (see Figure 8) that the transition occurs much like previously discussed. One of the disturbances gains energy and consequently slows down. It can clearly be seen that the weaker but faster disturbances behind it merge into the high amplitude wave. It can also be observed that the small amplitude wave in front speeds away from the high amplitude wave. The resulting wave pattern has a wavelength equal to the total domain width and exhibits strong offshore directed velocities.

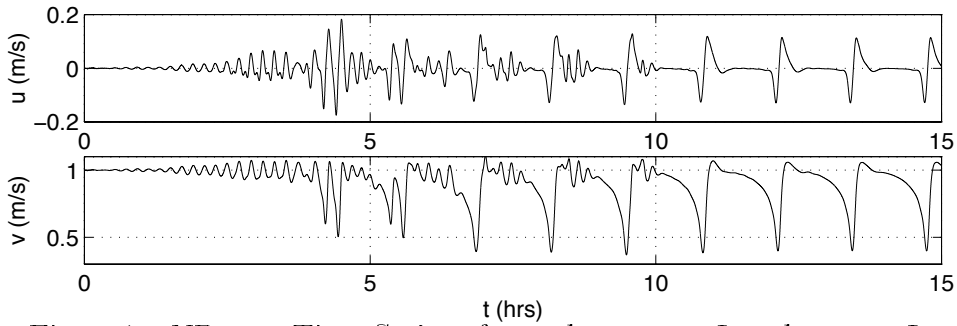

Figure 7: $ND = 4$, Time Series of u and v at $x = L$ and $y = 0.5L_y$

Summary and Future Work

In this study, a comprehensive model has been developed with the objective of studying low frequency motions in the surf and swash zones. This model has been used to study instabilities in the longshore current. Results are in quantitative agreement with the results by Allen *et al.* (1995) and in qualitative agreement with Falqués *et al.* (1994). As both studies incorporated the rigid lid assumption, the agreement of their results with the results of the present study confirms that the rigid lid approximation is valid.

It can be seen that the long term evolution of instabilities in the longshore current in the domain considered here is strongly dominated by subharmonic transitions. These transitions occur in the form of vortex pairing and subsequent reduction in the number of waves evident. The resulting flow structures are longshore progressive and exhibit strong offshore directed velocities. These results are intriguing and possibly suggestive of a mechanism for formation of migrating rip currents.

However, it is evident that the use of more realistic bottom topographies including bars and longshore non-uniformities is necessary to compare the trends in the results to observations. Also of interest are the interactions of these motions with other low frequency motions and the effect of longshore non-uniform forcing.

Acknowledgments The authors would like to thank Dr. Uday Putrevu for providing the software used to obtain the linear solutions. This research has been sponsored by the Office of Naval Research Coastal Sciences Program.

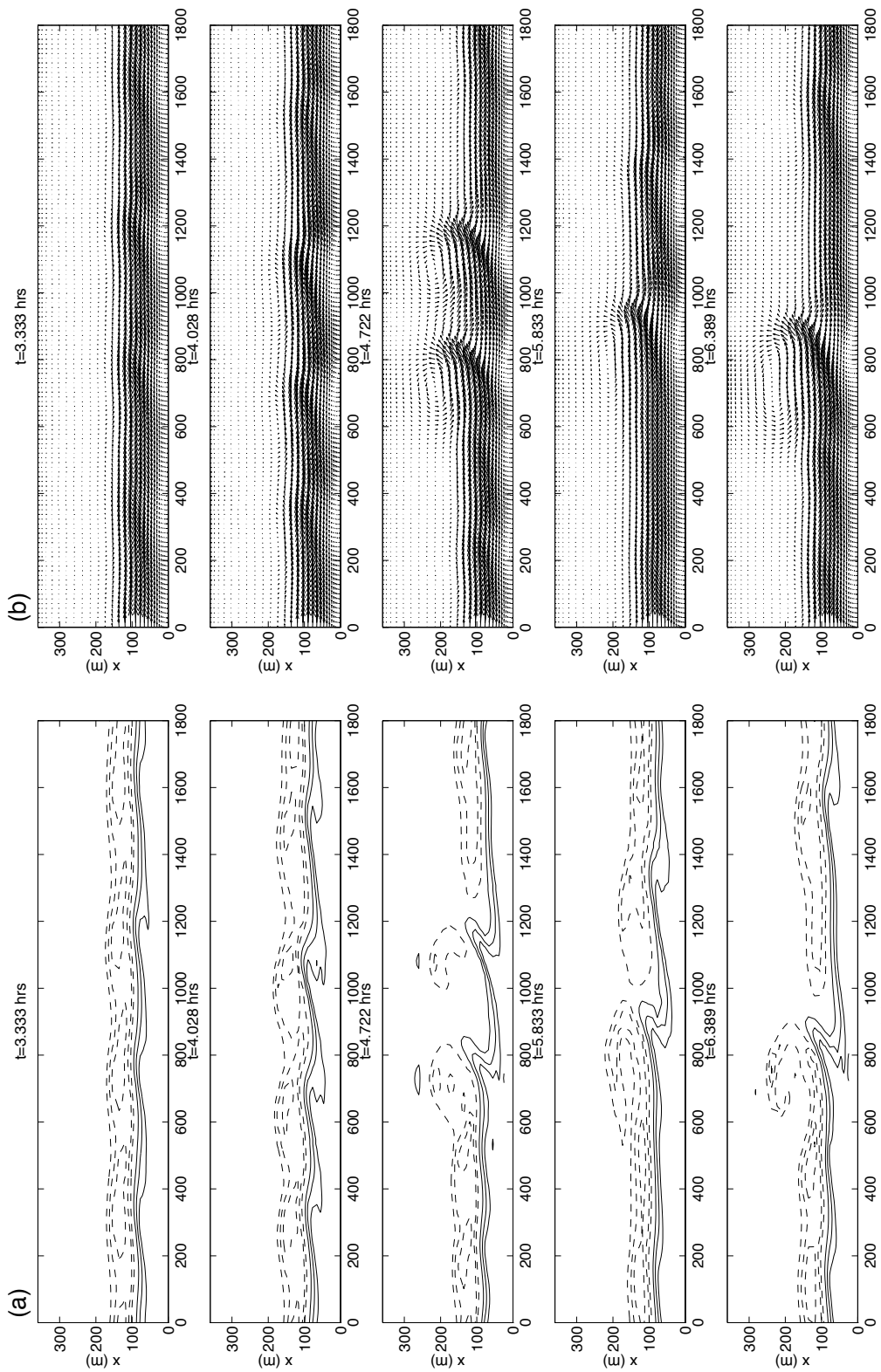

Figure 8: $ND = 4$, (a) Contour plot of potential vorticity (solid for $q > 0$, dashed for $q < 0$) (b) Circulation pattern

References

Allen, J., P.A. Newberger and R.A. Holman (1995). "Nonlinear shear instabilities of alongshore currents on plane beaches." manuscript.

Bowen, A.J. and R.A. Holman (1989). "Shear instabilities of the mean longshore current. 1. Theory." *J. Geophys. Res.*, 94, 18023-18030.

Carrier, G.F. and H.P. Greenspan (1958). "Water waves of finite amplitude on a sloping beach." *J. Fluid Mech.*, 4, *part 1*, pp. 97-109.

Dodd, N., J. Oltman-Shay and E.B. Thornton (1992). "Shear instabilities in the longshore current: A comparison of observation and theory." *J. Phys. Oceanog.*,22, 1, 62-82.

Dodd, N. and E.B. Thornton (1992). "Longshore current instabilities: Growth to finite amplitude." *Proc. 23rd Intl. Conf. Coastal Eng.*, Venice, 2655-2668.

Dodd, N. (1994). "On the destabilization of a longshore current on a plane beach: Bottom shear stress, critical conditions, and onset of stability." *J. Geophys. Res.*, 99, C1, 811-824.

Falqués, A. and V. Iranzo (1992). "Edge waves on a longshore shear flow." *Phys. Fluids A*, 4 (10), 2169-2190.

Falqués, A. and V. Iranzo (1994). "Numerical simulation of vorticity waves in the nearshore." *J. Geophys. Res.*, 99, C1, 825-841.

Falqués, A., V. Iranzo and M. Caballería (1994). "Shear instability of longshore currents: Effects of dissipation and nonlinearity." *Proc. 24th Intl. Conf. Coastal Eng.*, Kobe, 1983-1997.

Oltman-Shay, J., P.A. Howd and W.A. Birkemeier (1989). "Shear instabilities of the mean longshore current. 2. Field Observation." *J. Geophys. Res.*, 94, 18031-18042.

Putrevu, U. and I.A. Svendsen (1992). "Shear instability of longshore currents: A numerical study." *J. Geophys. Res.*, 97, C5, 7283-7303.

Reniers, A.J., J.A. Battjes, A. Falqués and D.A. Huntley (1994). "Shear wave laboratory experiment." *Proc. Intl. Symposium: Waves - Physical and numerical modeling*, vol.1, Vancouver, 356-365.

Van Dongeren, A.R., F.E. Sancho, I.A. Svendsen and U. Putrevu (1994). "SHORECIRC: A quasi 3-D nearshore model." *Proc. 24th Intl. Conf. Coastal Eng.*, Kobe, 2741-2754.

Zelt, J.A. (1986). "Tsunamis: The response of harbours with sloping boundaries to long wave excitation." Report No. KH-R-47, California Institute of Technology, Pasadena, California.